Synthesis, photophysical and biological properties of tricarbonyl Re(I) diimine complexes bound to thiotetrazolato ligands

Liam J. Stephens[#], Elena Dallerba[#], Jenisi T.A. Kelderman, Aviva Levina, Melissa V. Werrett, Peter A. Lay, Massimiliano Massi[*] and Philip C. Andrews[*]

NMR Details

Collated ^{1}H and ^{13}C NMR Spectra of all Re complexes (Figures S1-S24)

Crystallography Details

Tabulated data for crystal structures of **RebipyLn** and **RephenLn** (Table S1)

Molecular structure of selected complexes (Figures S25 - Figure S34)

Powder X-ray diffraction

PXRD for complex **RebipyL4** (Figure S35)

Stability Studies

Stability of **RephenL2** in DMSO (Figure S36)

RebipyL1

Figure S1. ^{1}H NMR for [Re(bipy)(CO)$_3$(L1)], **RebipyL1**

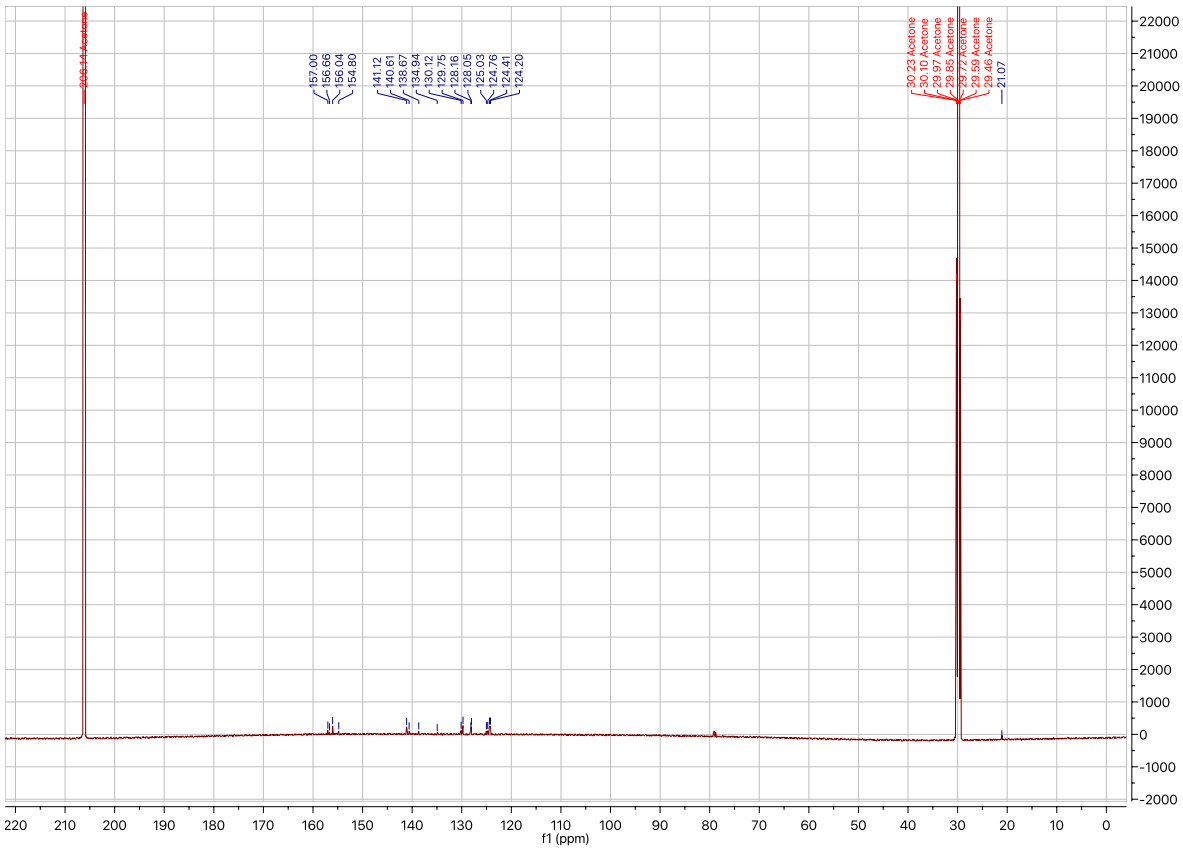

Figure S2. ^{13}C NMR for [Re(bipy)(CO)$_3$(L1)], **RebipyL1**

RebipyL2

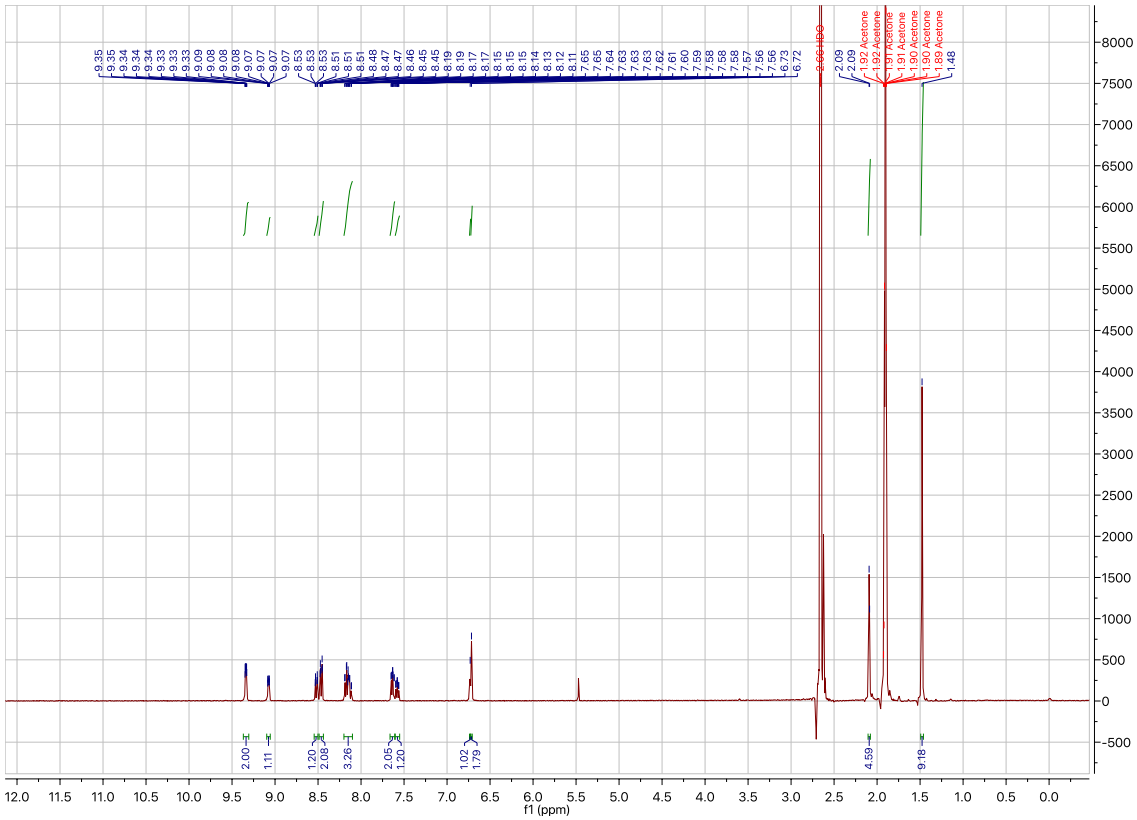

Figure S3. ^{1}H NMR for [Re(bipy)(CO)$_3$(L2)], **RebipyL2**

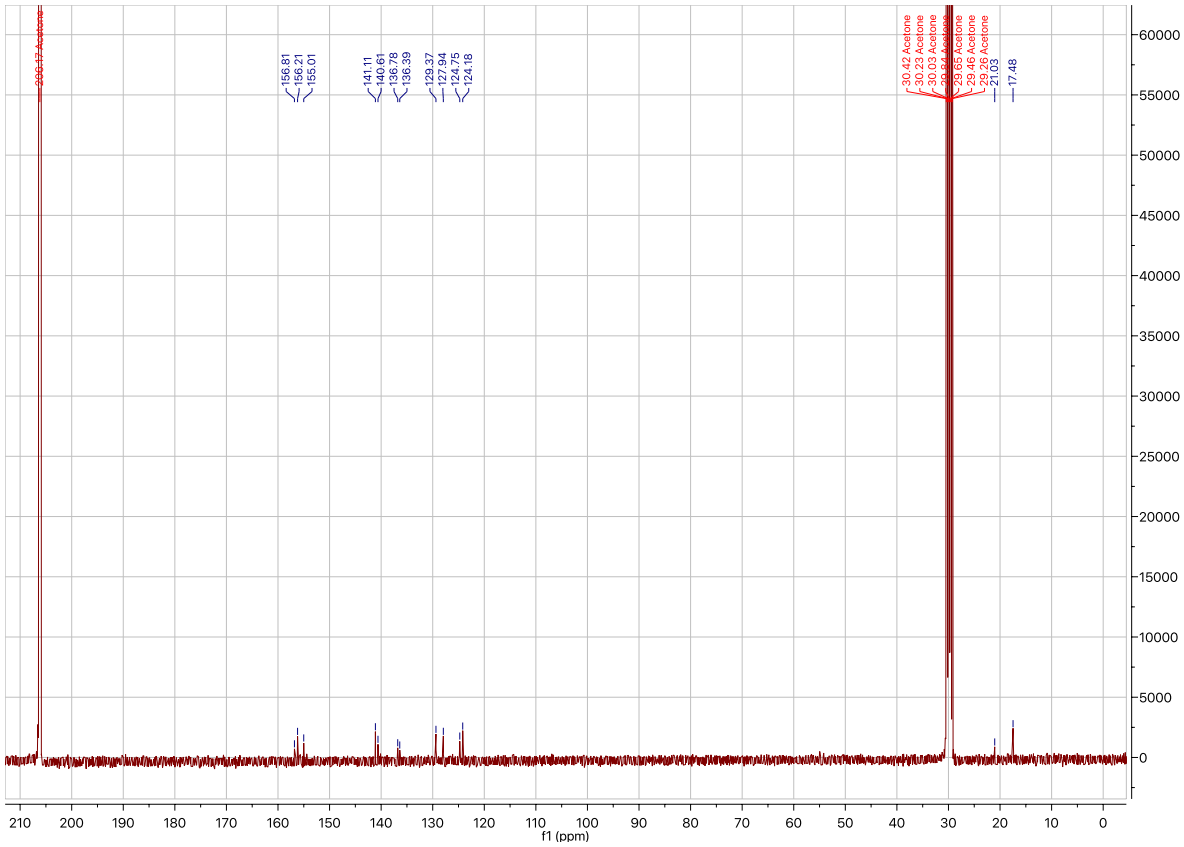

Figure S4. ^{13}C NMR for [Re(bipy)(CO)$_3$(L2)], **RebipyL2**

RebipyL3

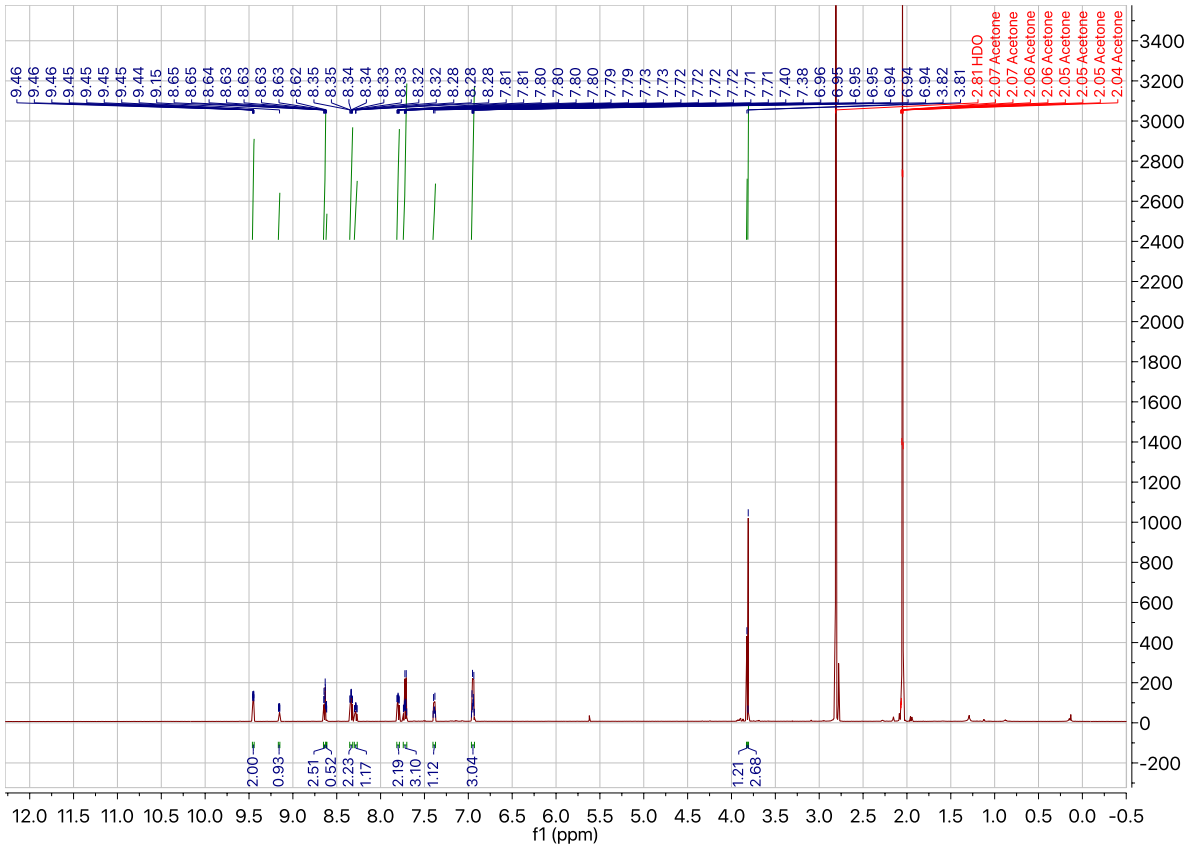

Figure S5. ^{1}H NMR for [Re(bipy)(CO)$_3$(L3)], **RebipyL3**

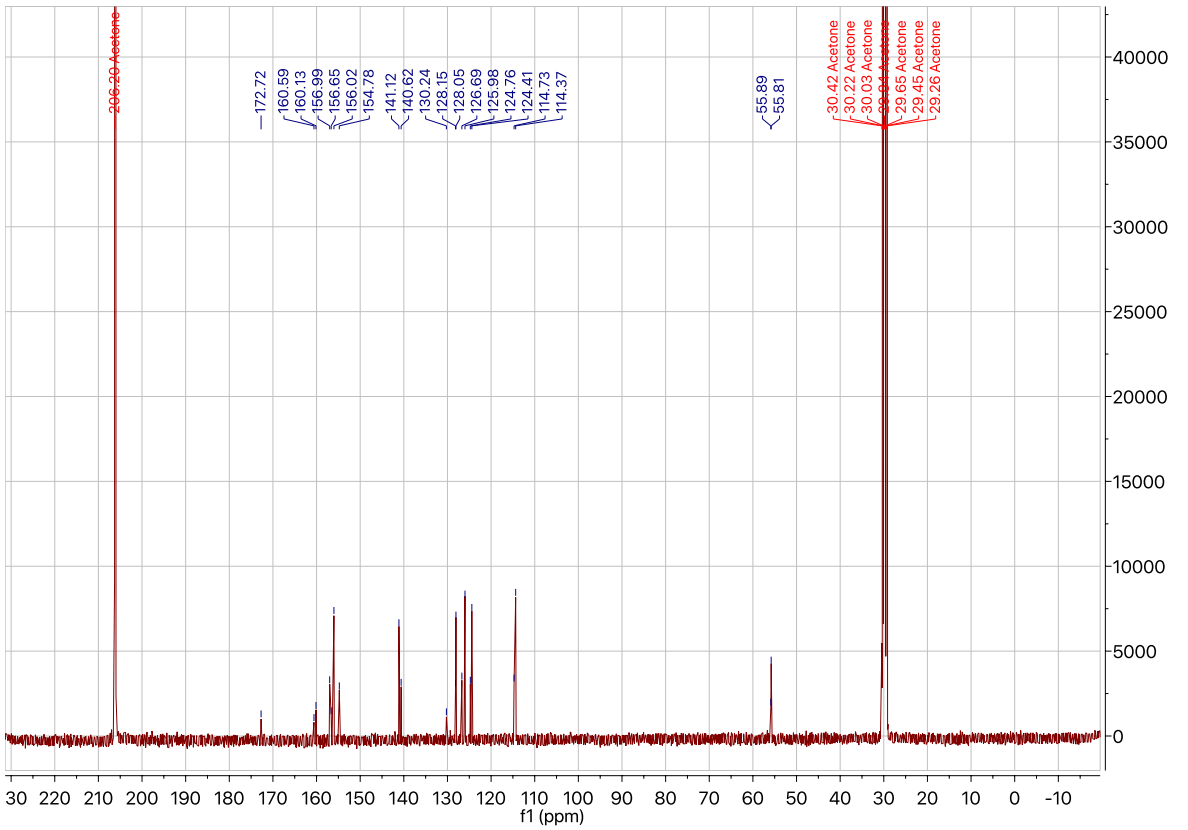

Figure S6. ^{13}C NMR for [Re(bipy)(CO)$_3$(L3)], **RebipyL3**

RebipyL4

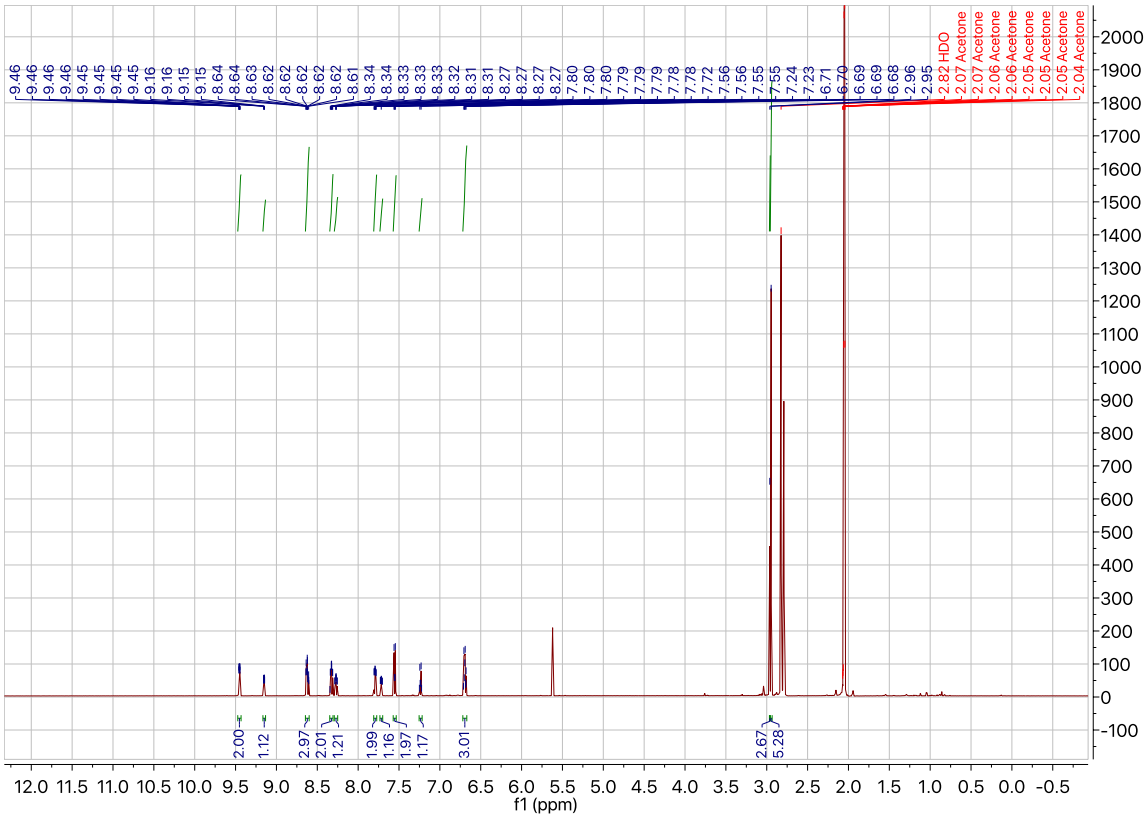

Figure S7. ^{1}H NMR for [Re(bipy)(CO)$_3$(L4)], **RebipyL4**

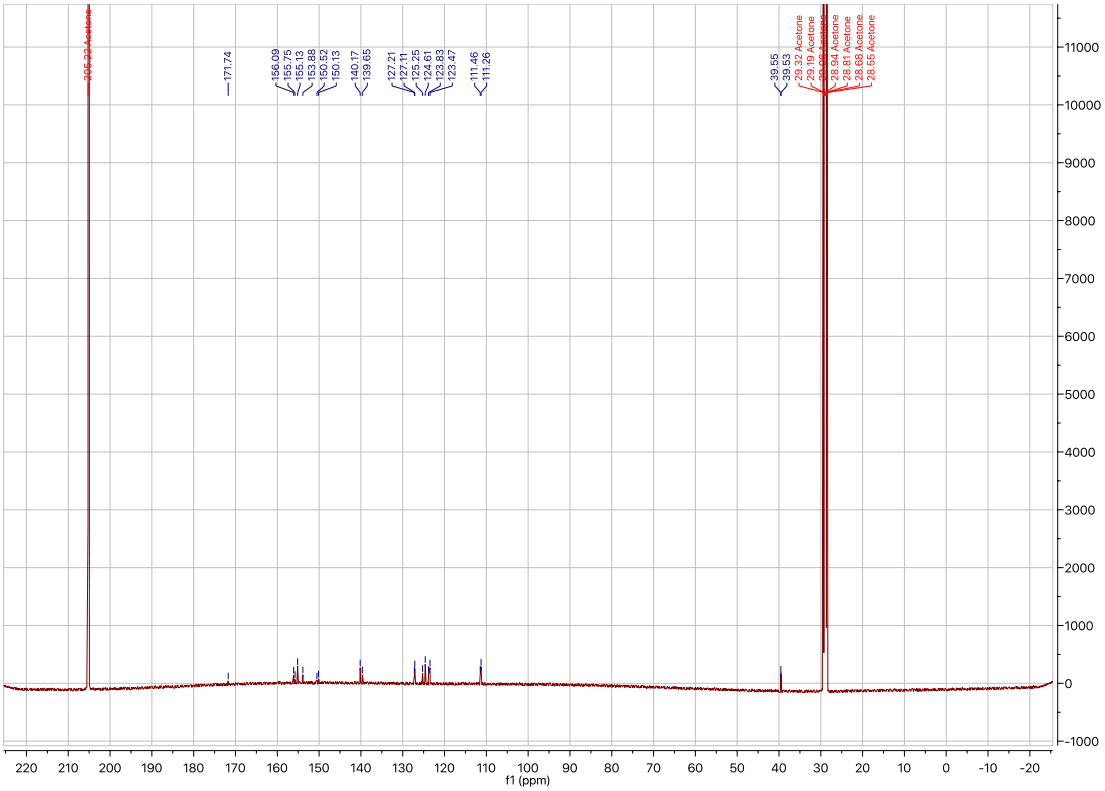

Figure S8. ^{13}C NMR for [Re(bipy)(CO)$_3$(L4)], **RebipyL4**

RebipyL5

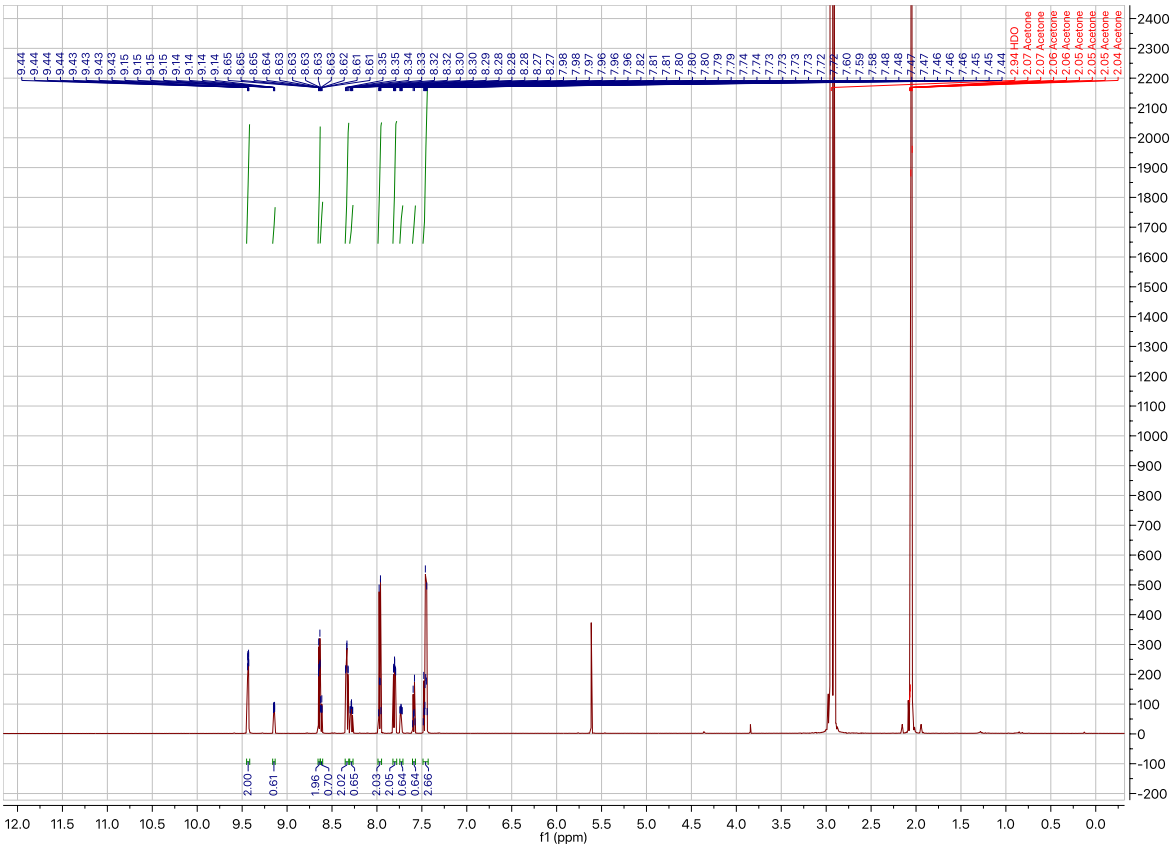

Figure S9. ^{1}H NMR for [Re(bipy)(CO)$_3$(L5)], **RebipyL5**

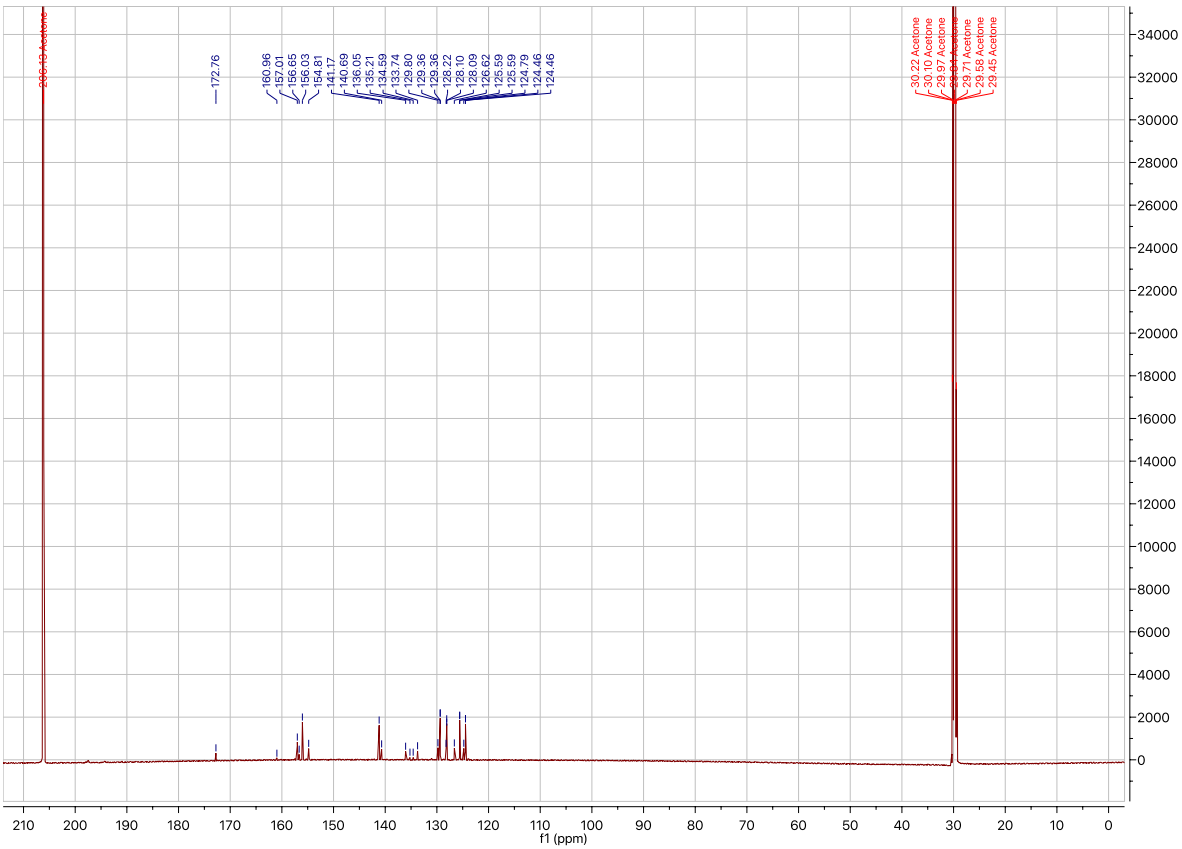

Figure S10. ^{13}C NMR for [Re(bipy)(CO)$_3$(L5)], **RebipyL5**

RebipyL6

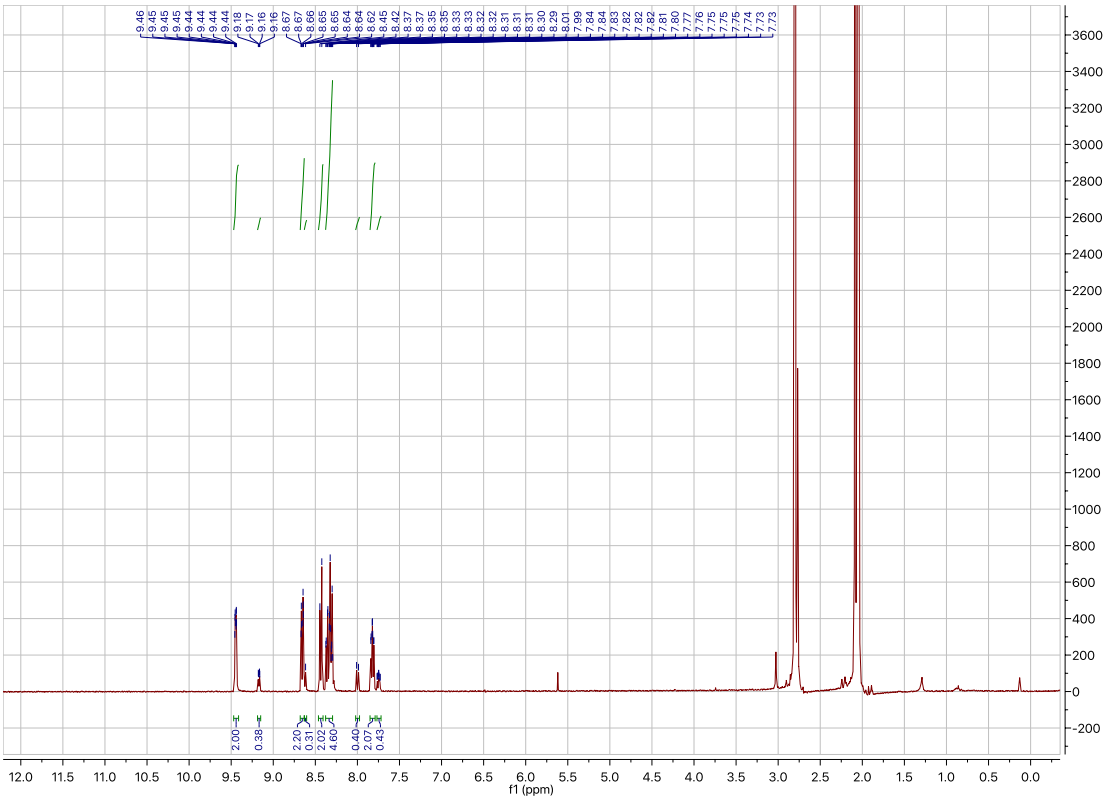

Figure S11. ^{1}H NMR for [Re(bipy)(CO)$_3$(L6)], **RebipyL6**

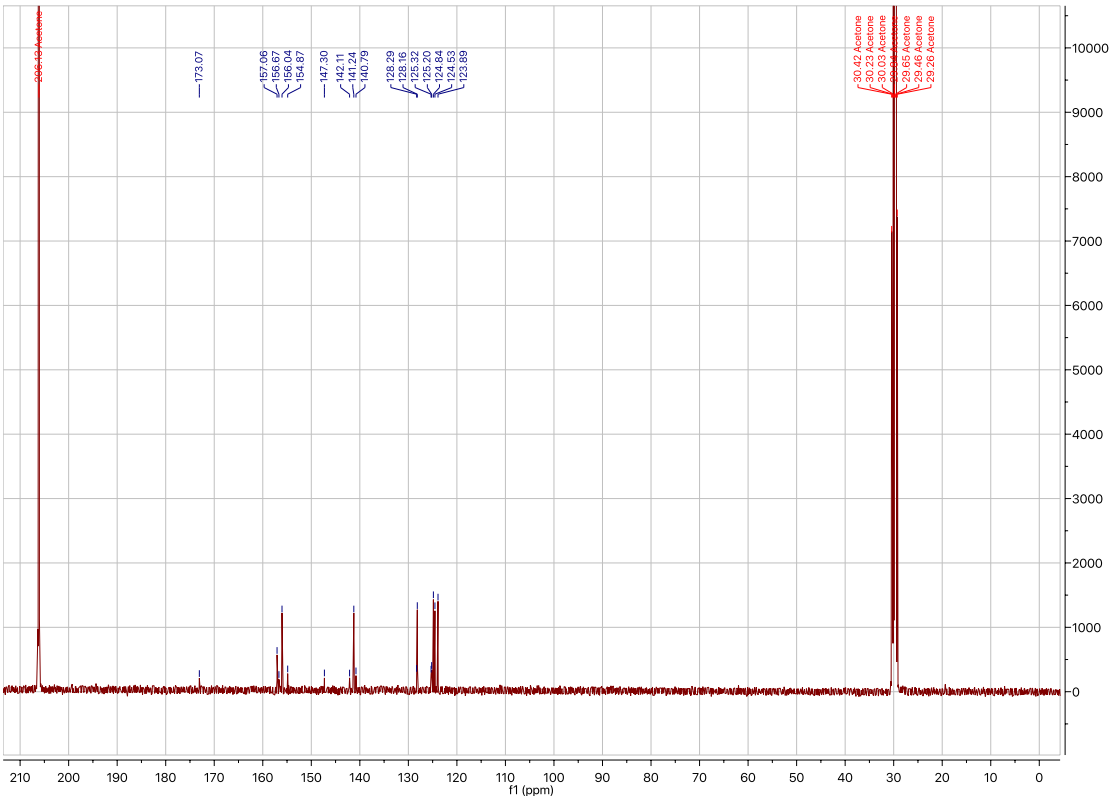

Figure S12. ^{13}C NMR for [Re(bipy)(CO)$_3$(L6)], **RebipyL6**

RephenL1

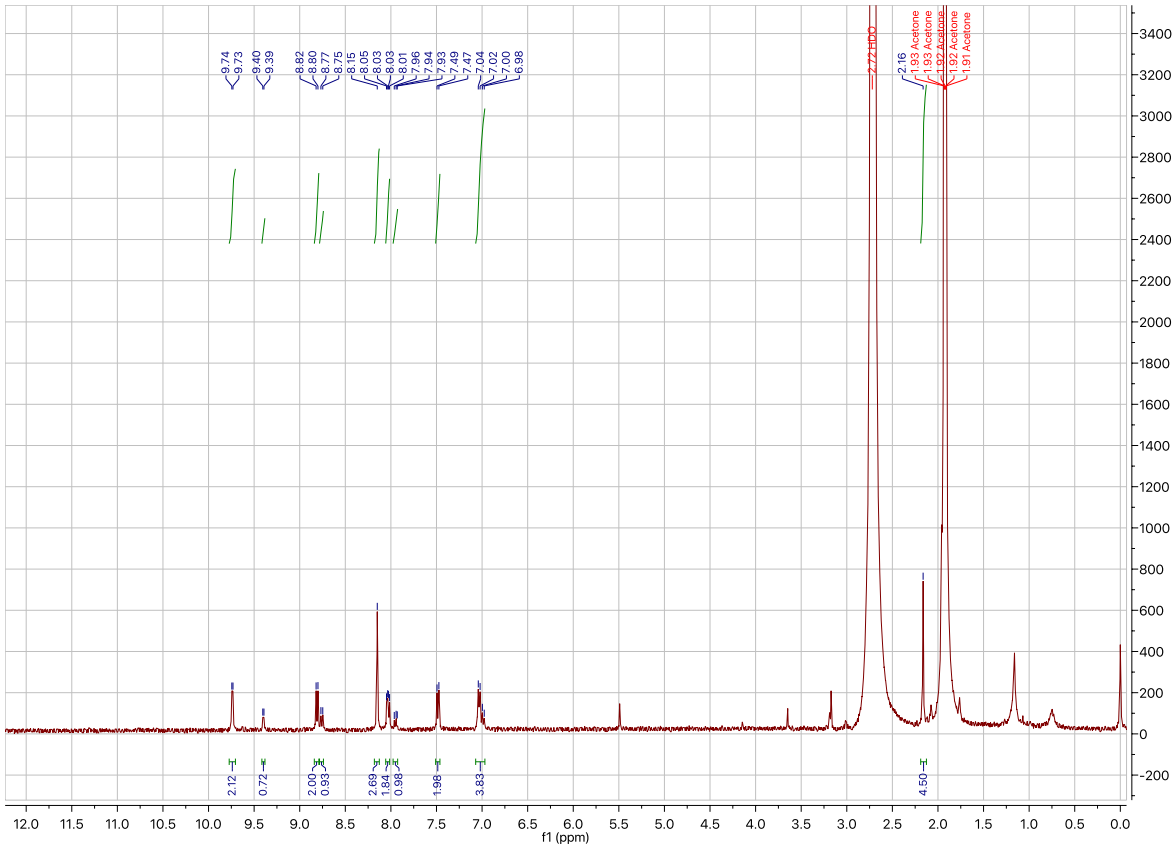

Figure S13. ^{1}H NMR for [Re(phen)(CO)$_3$(L1)], **RephenL1**

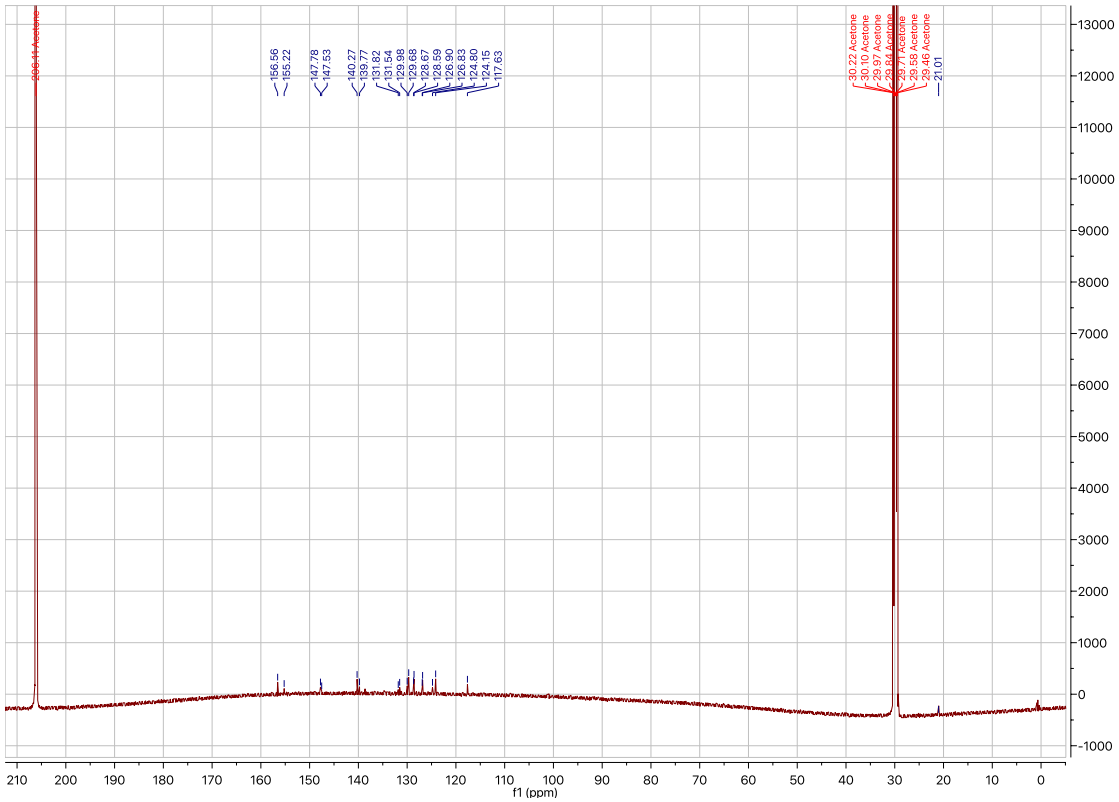

Figure S14. ^{13}C NMR for [Re(phen)(CO)$_3$(L1)], **RephenL1**

RephenL2

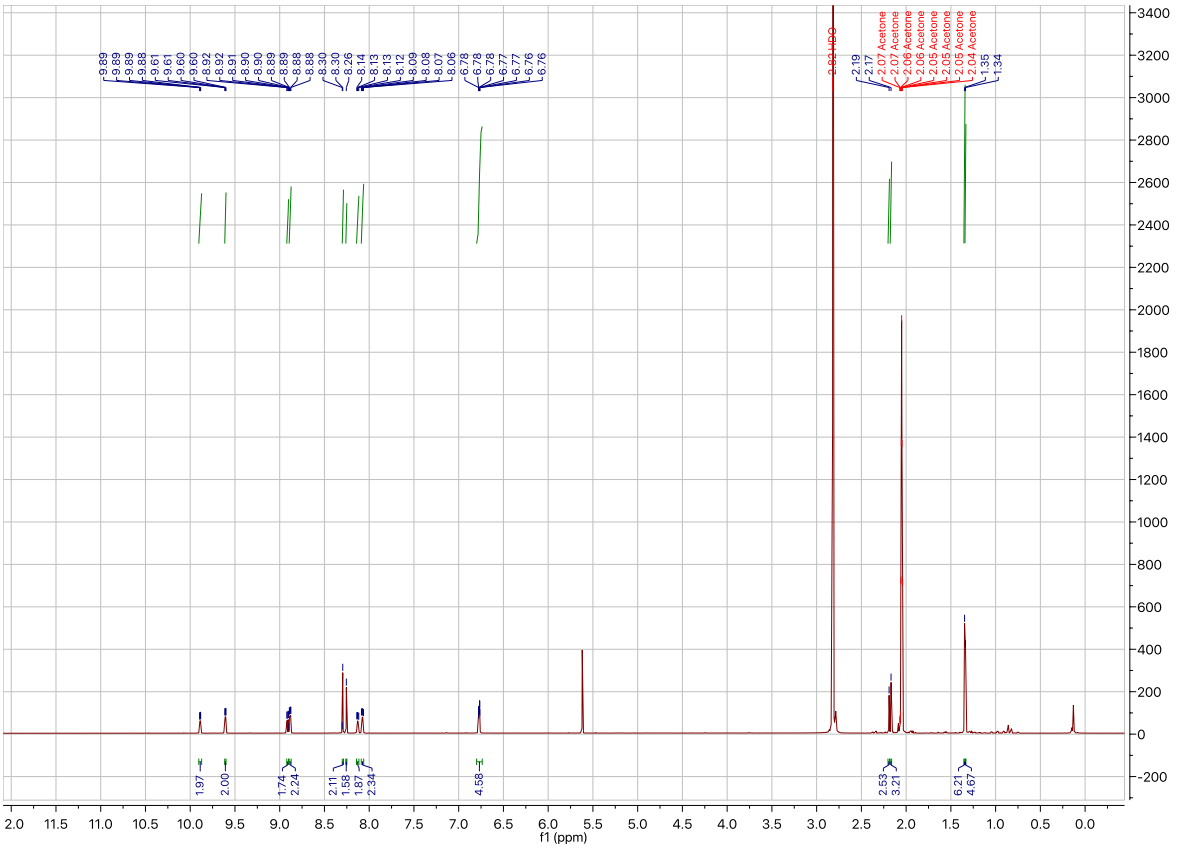

Figure S15. ^{1}H NMR for [Re(phen)(CO)$_3$(L2)], **RephenL2**

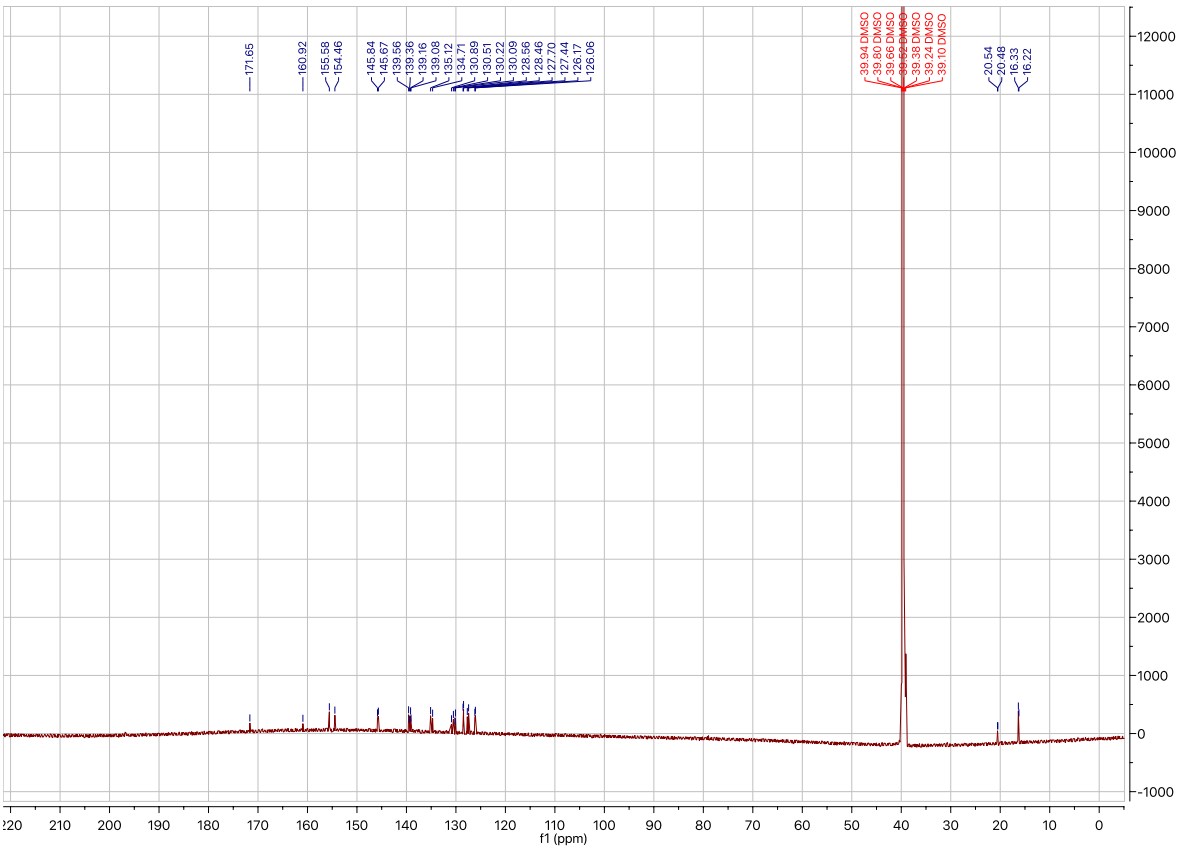

Figure S16. ^{13}C NMR for [Re(phen)(CO)$_3$(L2)], **RephenL2**

RephenL3

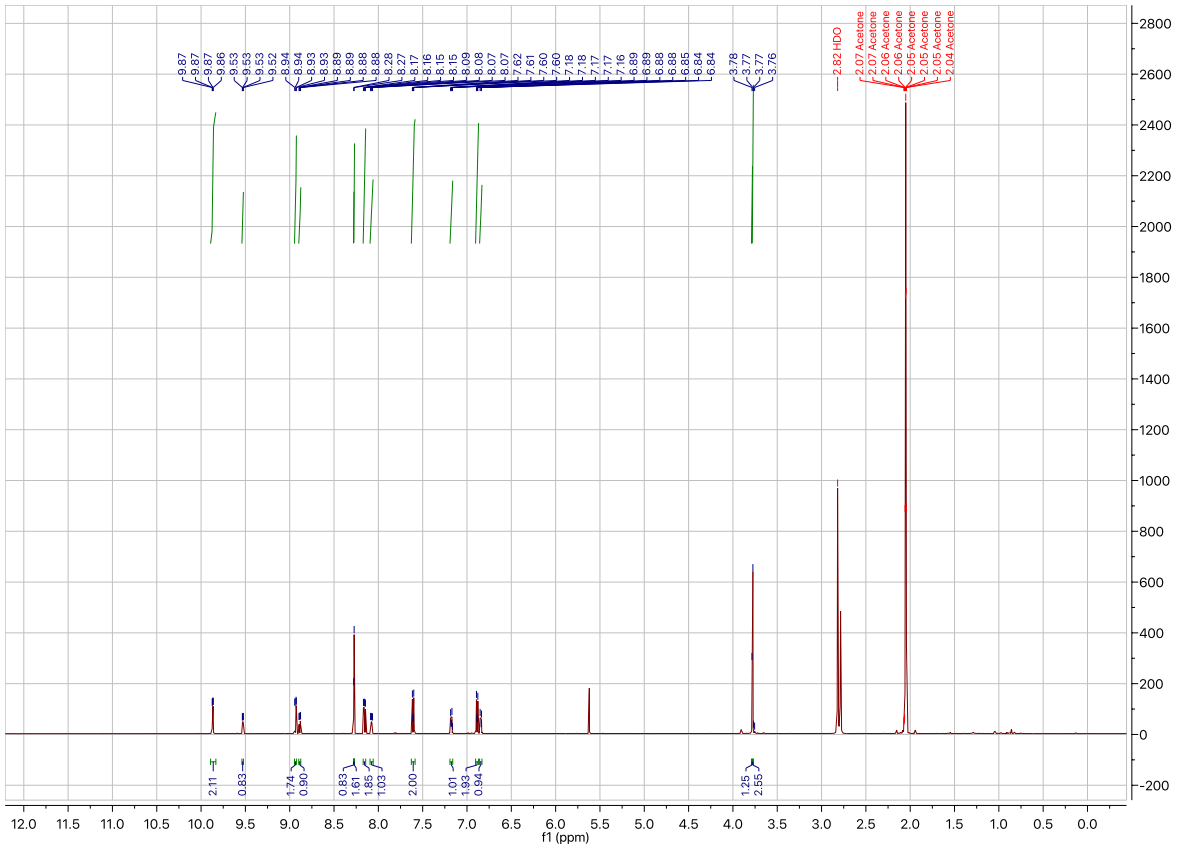

Figure S17. ^{1}H NMR for [Re(phen)(CO)$_3$(L3)], **RephenL3**

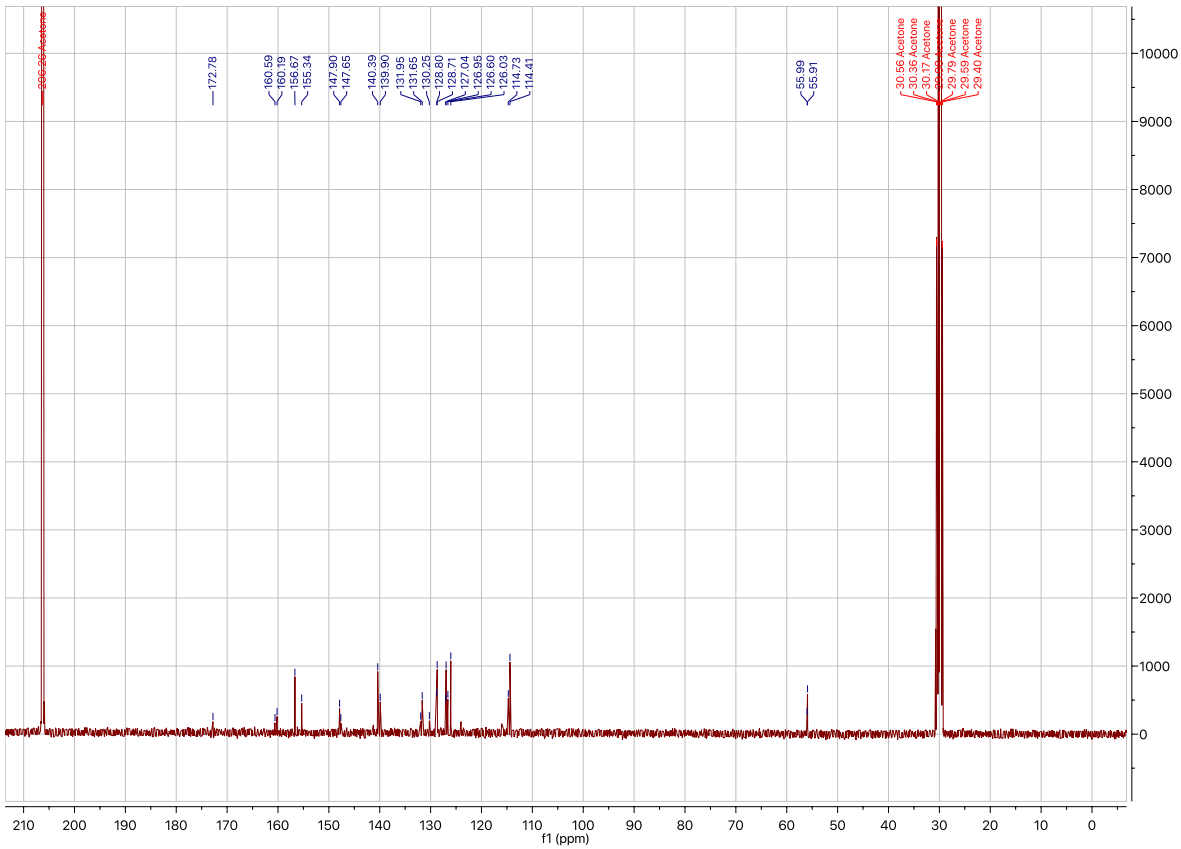

Figure S18. ^{13}C NMR for [Re(phen)(CO)$_3$(L3)], **RephenL3**

RephenL4

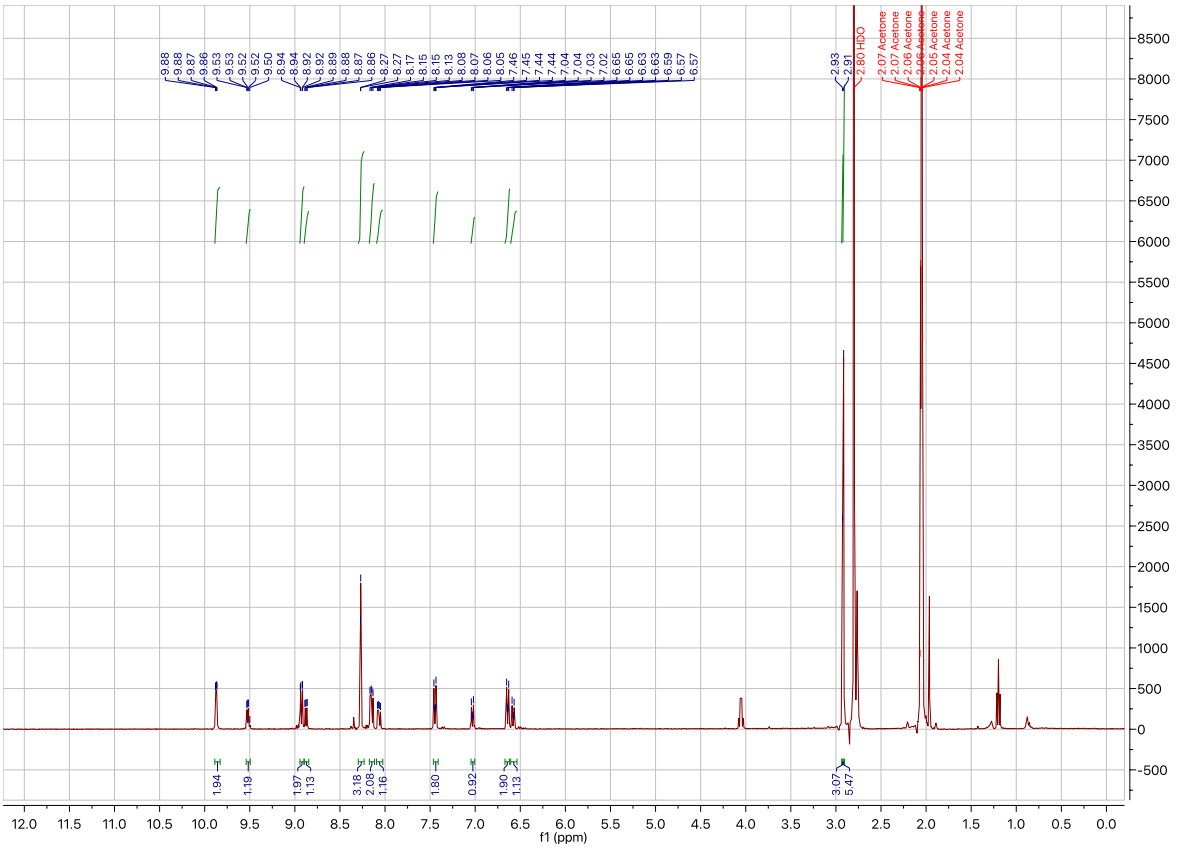

Figure S19. ^{1}H NMR for [Re(phen)(CO)$_3$(L4)], **RephenL4**

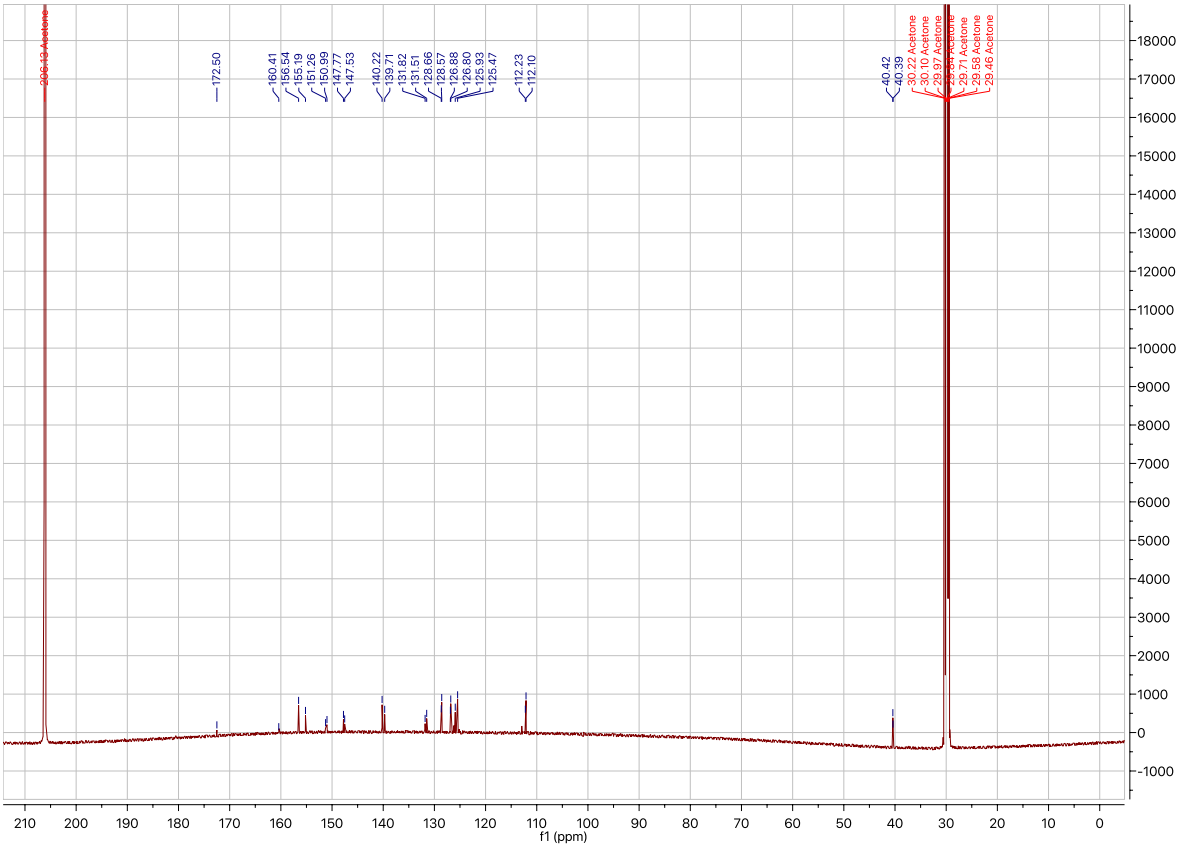

Figure S20. ^{13}C NMR for [Re(phen)(CO)$_3$(L4)], **RephenL4**

RephenL5

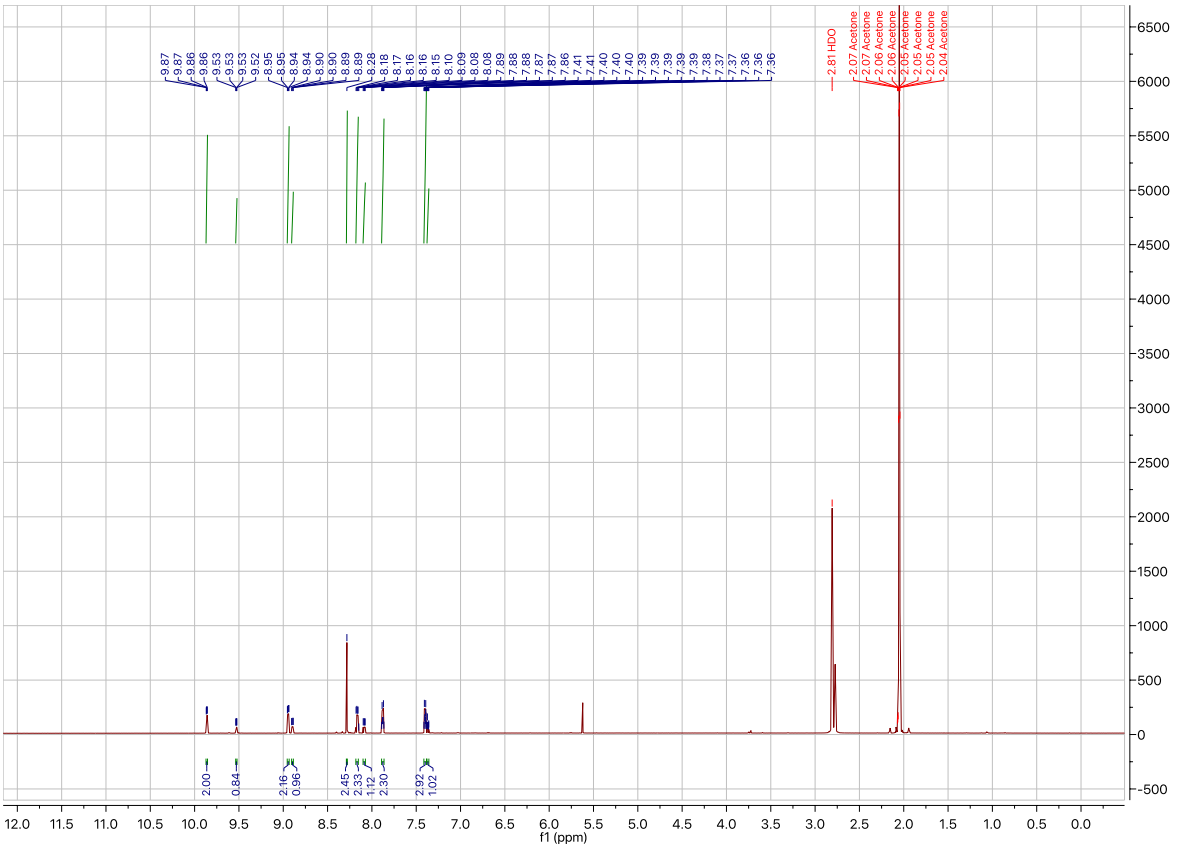

Figure S21. ^{1}H NMR for [Re(phen)(CO)$_3$(L5], **RephenL5**

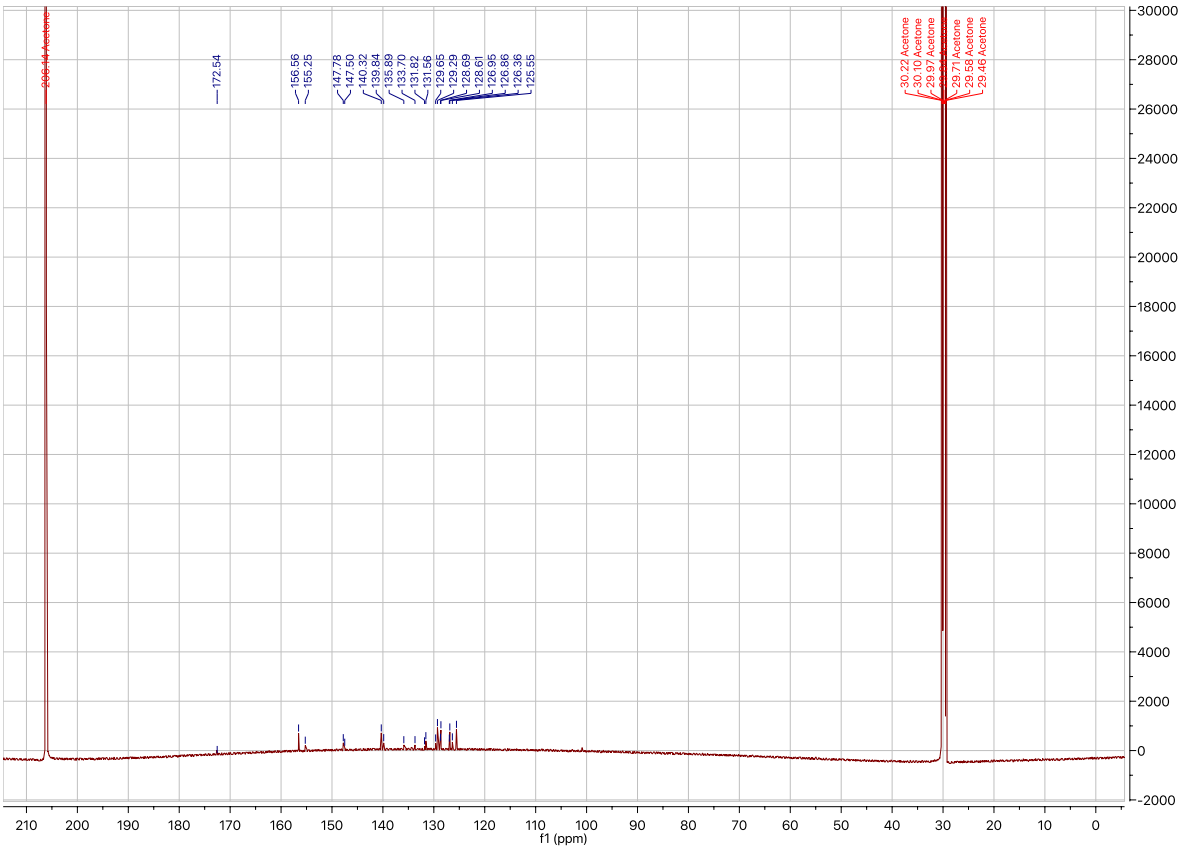

Figure S22. ^{13}C NMR for [Re(phen)(CO)$_3$(L5], **RephenL5**

RephenL6

Figure S23. ^{1}H NMR for [Re(phen)(CO)$_3$(L6], **RephenL6**

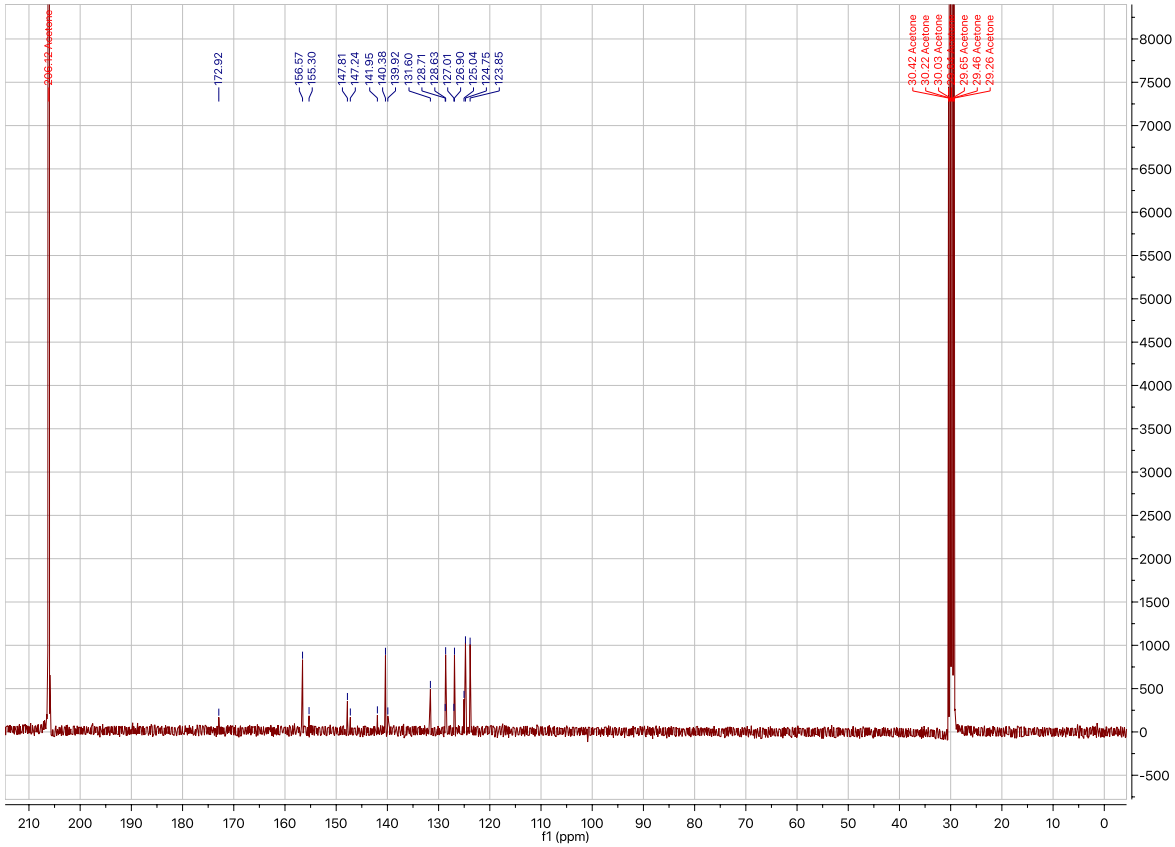

Figure S24. ^{13}C NMR for [Re(phen)(CO)$_3$(L6], **RephenL6**

Table S1. Crystallographic data for complexes **RebipyLn - RephenLn**

	Rebipy1	**RebipyL2**	**RebipyL3**	**RebipyL4**	**RebipyL5**	**RebipyL6**
Chemical formula	$C_{21}H_{15}N_6O_3ReS$	$C_{26}N_6O_4ReS_2$	$C_{21}H_{15}N_6O_4ReS$	$C_{22}H_{18}N_7O_3ReS$	$C_{23}H_{16}ClN_6O_4ReS$	$C_{23}H_{18}N_7O_6ReS$
M_r	617.65	698.64	633.65	646.69	694.13	706.70
Temp (K)	123	123	123	123	123	123
Crystal system, space group	Monoclinic, P $2_1/c$	Triclinic, P -1	Orthorhombic, pccn	Monoclinic, P $2_1/c$	Orthorhombic, P2_1ca	Orthorhombic, P2_1ca
a,b,c (Å)	19.8643(10) 9.4378(3) 11.9223(6)	10.1365(2) 11.5551(2) 12.4450(3)	19.7329(7) 18.0795(7) 12.6323(4)	21.2128(12) 9.4134(4) 11.9069(6)	12.9404(5) 9.4757(3) 20.6156(8)	12.8312(4) 9.5879(3) 20.5152(5)
V	2159.87(18)	1388.02(5)	4506.7(3)	2306.9(2)	2527.87(16)	2523.87(13)
Z	4	2	8	4	4	4
Wr²	0.1302	0.0838	0.1063	0.0999	0.0932	0.0827
GOF	0.992	0.992	1.023	1.008	1.048	1.032
No. of reflections	5487	6817	5924	5076	6320	8397
No. of parameters	343	343	302	377	326	345

	RephenL1	**RephenL2**	**RephenL3**	**RephenL4**	**RephenL5**	**RephenL6**
Chemical formula	$C_{23}H_{15}N_6O_3ReS$	$C_{25}H_{19}N_6O_3ReS$	$C_{23}H_{15}N_6O_4ReS$	$C_{24}H_{15}N_7O_3ReS.$ $0.5(C_3H_6O)$	$C_{22}H_{12}ClN_6O_3ReS$	$C_{25}H_{18}N_7O6ReS$
M_r	641.67	669.72	657.67	696.73	662.09	730.72
Temp (K)	123	123	123	123	123	123
Crystal system, space group	Monoclinc, P $2_1/c$	Monoclinc, P $2_1/c$	Orthorhombic, P 2_1 2_1 2_1	Triclinic, P -1	Monoclinc, P $2_1/c$	Orthorhombic, P2_1ca
a,b,c (Å)	11.6710(3) 13.1288(4) 14.2480(4)	14.3598(10) 11.2264(6) 15.8108(9)	11.5391(3) 13.2808(3) 14.9093(4)	6.79070(10) 9.3555(2) 19.8603(3)	7.3952(2) 17.0085(6) 17.8443(6)	22.6481(11) 7.2466(3) 15.5837(9)
V	2182.95(11)	2375.3(3)	2284.83(10)	1244.72(4)	2200.10(12)	2557.6(2)
Z	4	4	4	2	4	4
Wr²	0.0678,	0.0909	0.0539	0.0734	0.0808	0.1004
GOF	1.038	0.992	0.999	0.982	1.025	1.019
No. of reflections	7669	5771	8720	13426	8699	4802
No. of parameters	308	328	318	359	307	363

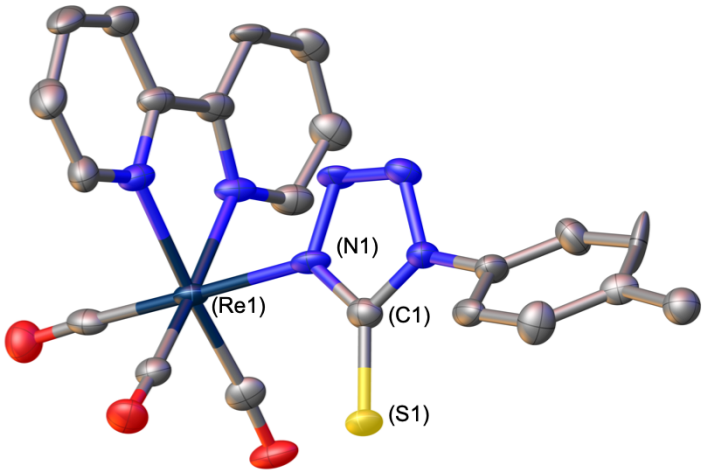

Figure S25. Molecular structure of **RebipyL1**, showing the N1 bound tetrazole. Hydrogen atoms omitted for clarity. Thermal ellipsoids shown at 50% probability.

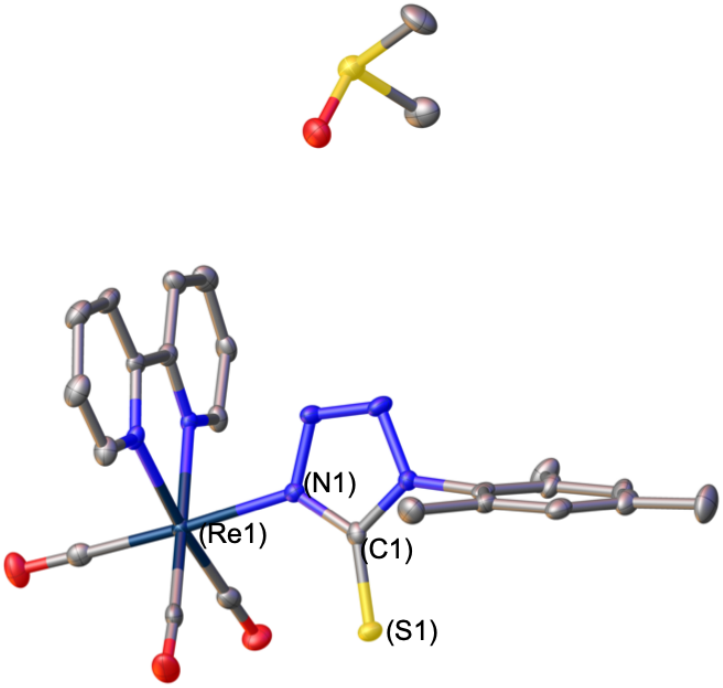

Figure S26. Molecular structure of **RebipyL2**, showing the N1 bound tetrazole. Hydrogen atoms omitted for clarity. Thermal ellipsoids shown at 50% probability.

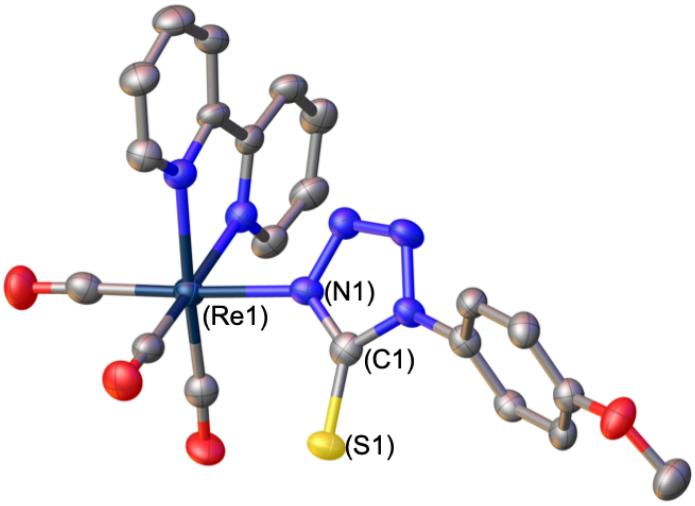

Figure S27. Molecular structure of **RebipyL3**, showing the N1 bound tetrazole. Hydrogen atoms omitted for clarity. Thermal ellipsoids shown at 50% probability.

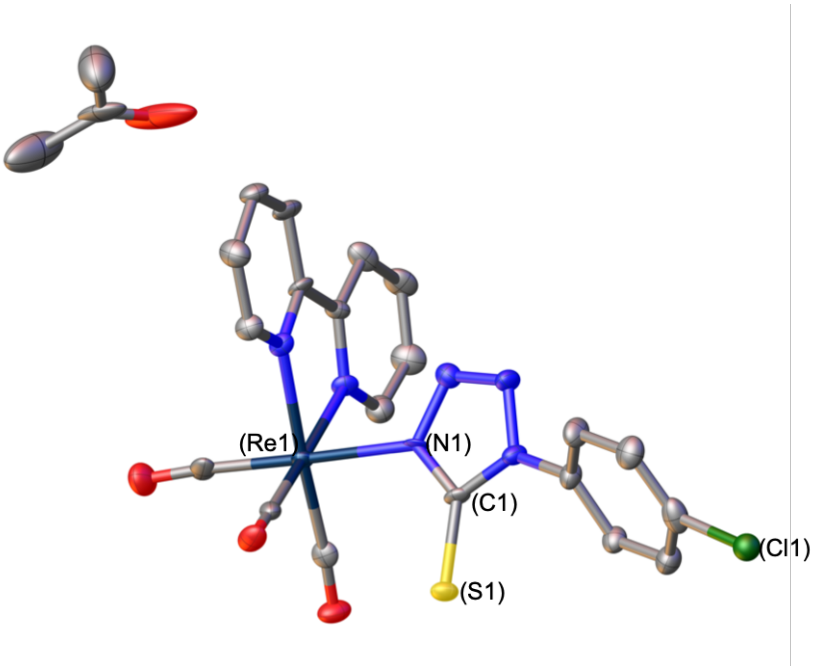

Figure S28. Molecular structure of **RebipyL5**, showing the N1 bound tetrazole. Hydrogen atoms omitted for clarity. Thermal ellipsoids shown at 50% probability.

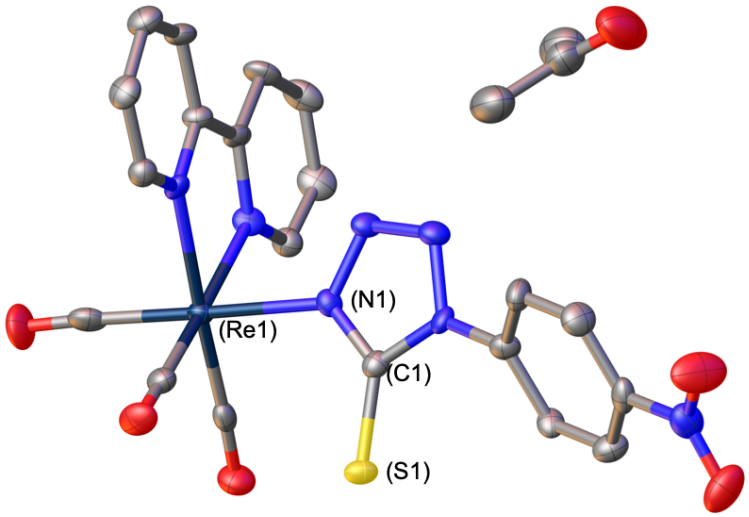

Figure S29. Molecular structure of **RebipyL6**, showing the N1 bound tetrazole. Hydrogen atoms omitted for clarity. Thermal ellipsoids shown at 50% probability.

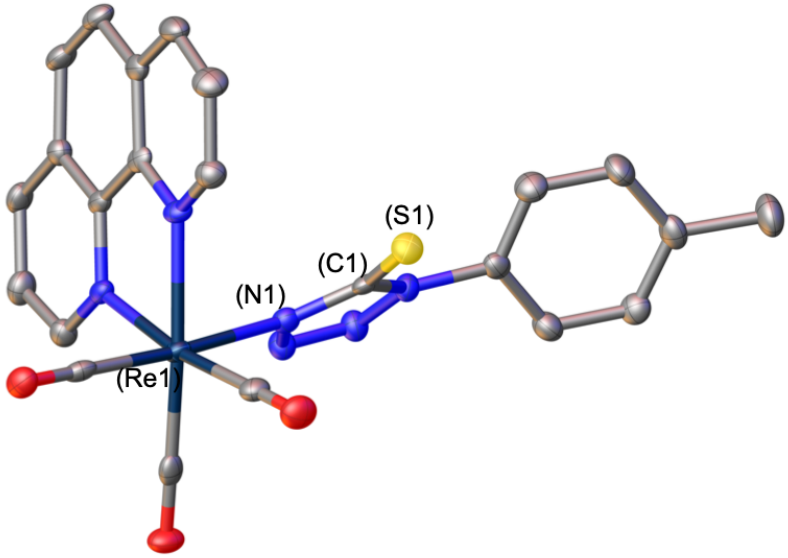

Figure S30. Molecular structure of **RephenL1**, showing the N1 bound tetrazole. Hydrogen atoms omitted for clarity. Thermal ellipsoids shown at 50% probability.

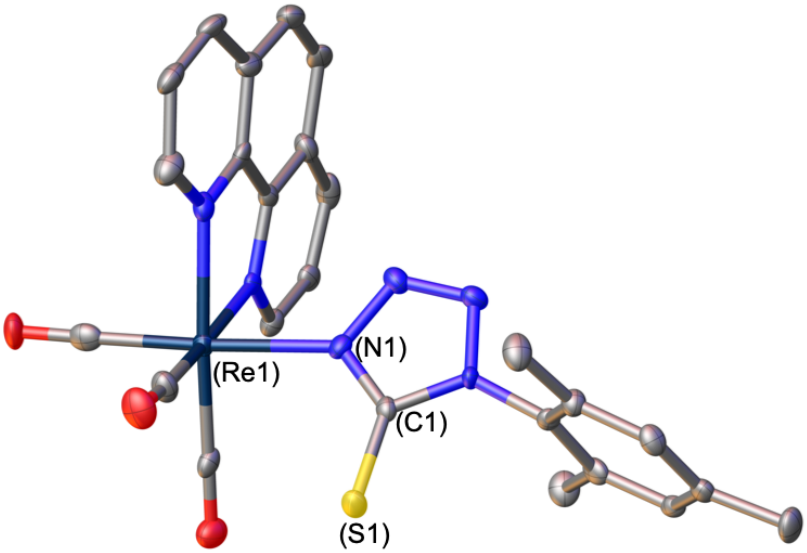

Figure S31. Molecular structure of **RephenL2**, showing the N1 bound tetrazole. Hydrogen atoms omitted for clarity. Thermal ellipsoids shown at 50% probability.

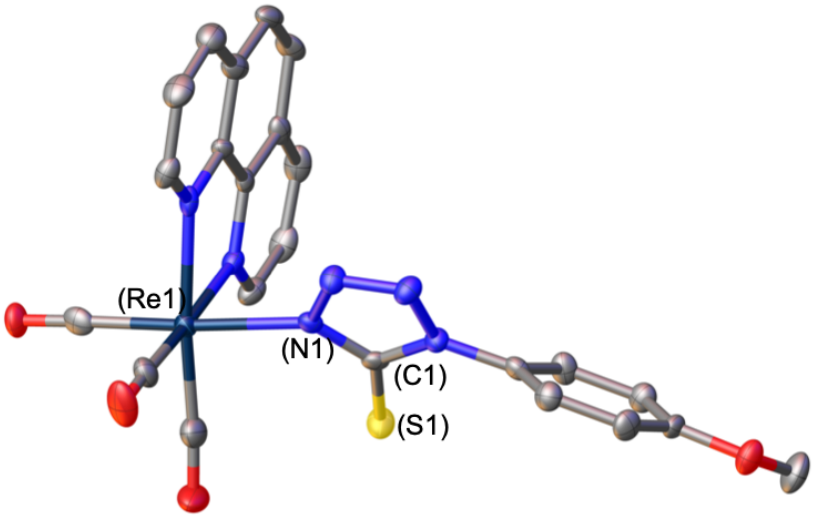

Figure S32. Molecular structure of **RephenL3**, showing the N1 bound tetrazole. Hydrogen atoms omitted for clarity. Thermal ellipsoids shown at 50% probability.

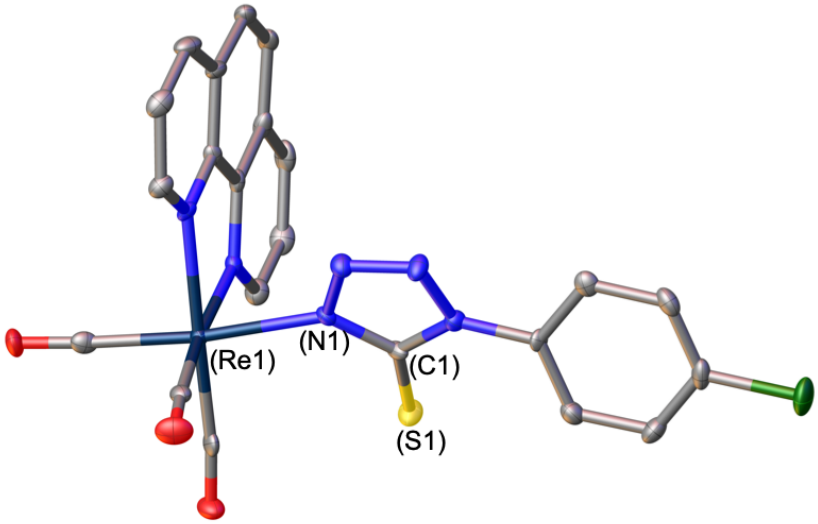

Figure S33. Molecular structure of **RephenL5**, showing the N1 bound tetrazole. Hydrogen atoms omitted for clarity. Thermal ellipsoids shown at 50% probability.

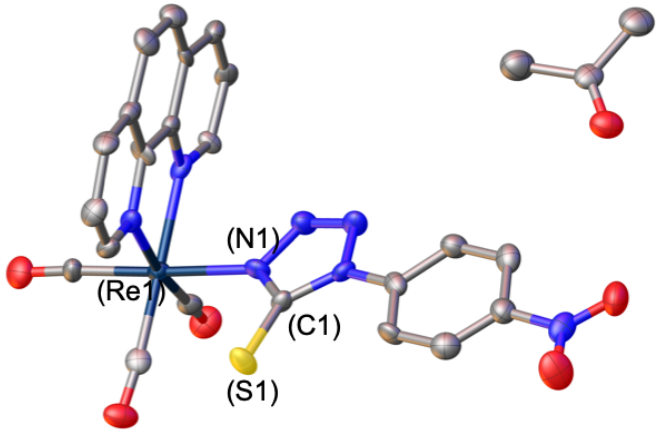

Figure S34. Molecular structure of **RephenL6**, showing the N1 bound tetrazole. Hydrogen atoms omitted for clarity. Thermal ellipsoids shown at 50% probability.

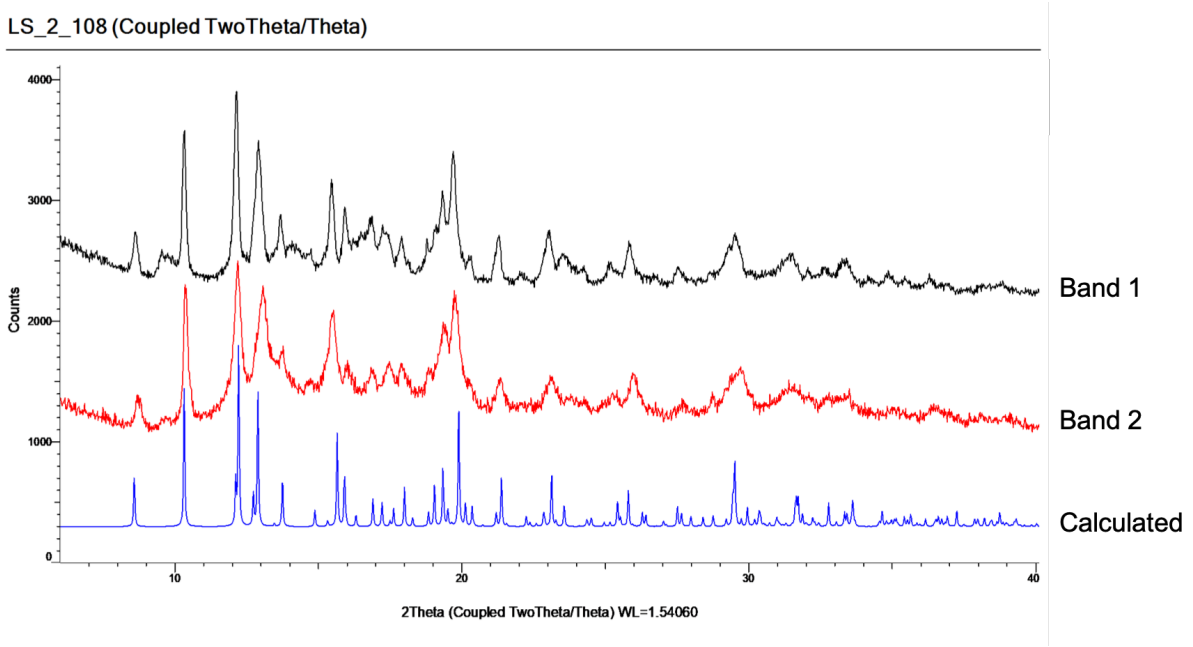

Figure S35. PXRD spectra for **RebipyL4**. Top (in black): solid material obtained in 'band one' from silica gel chromatography column; Middle (in red): solid material obtained in 'band two' from silica gel chromatography column; bottom (in blue): calculated PXRD using the crystal data obtained for **RebipyL4**.

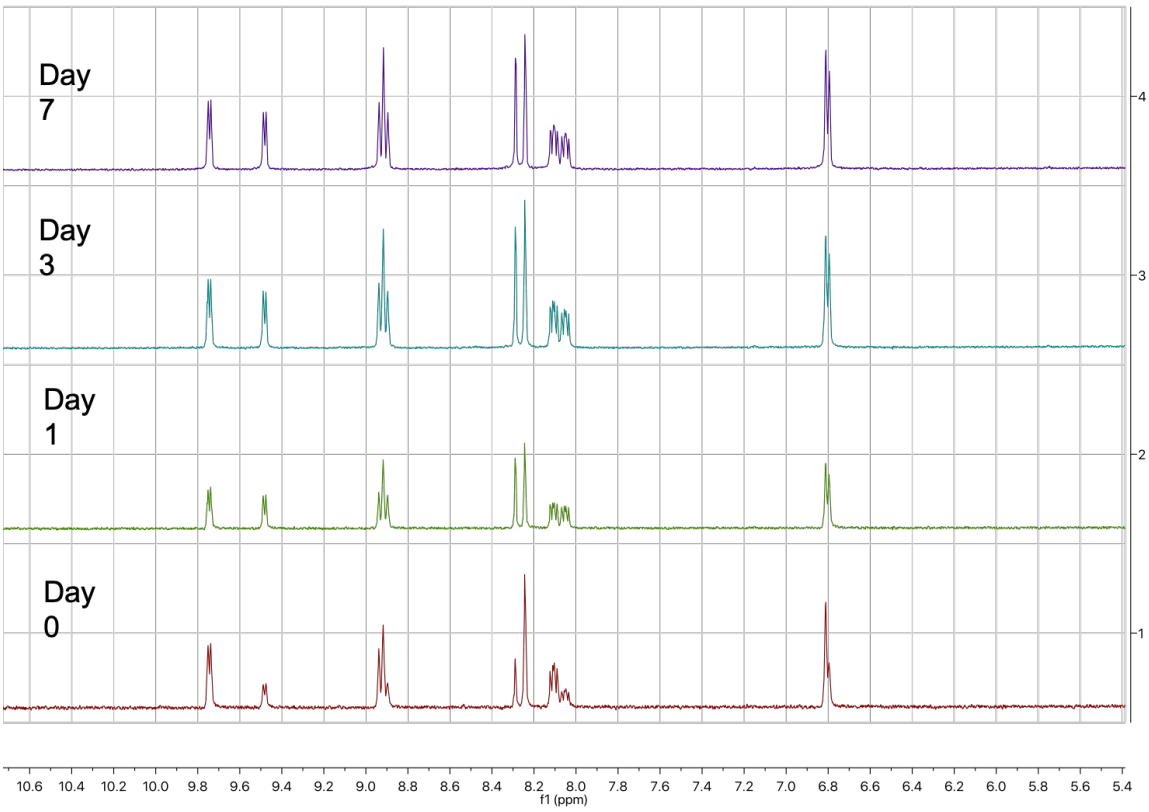

Figure S36. **RephenL2** seven-day stability in DMSO

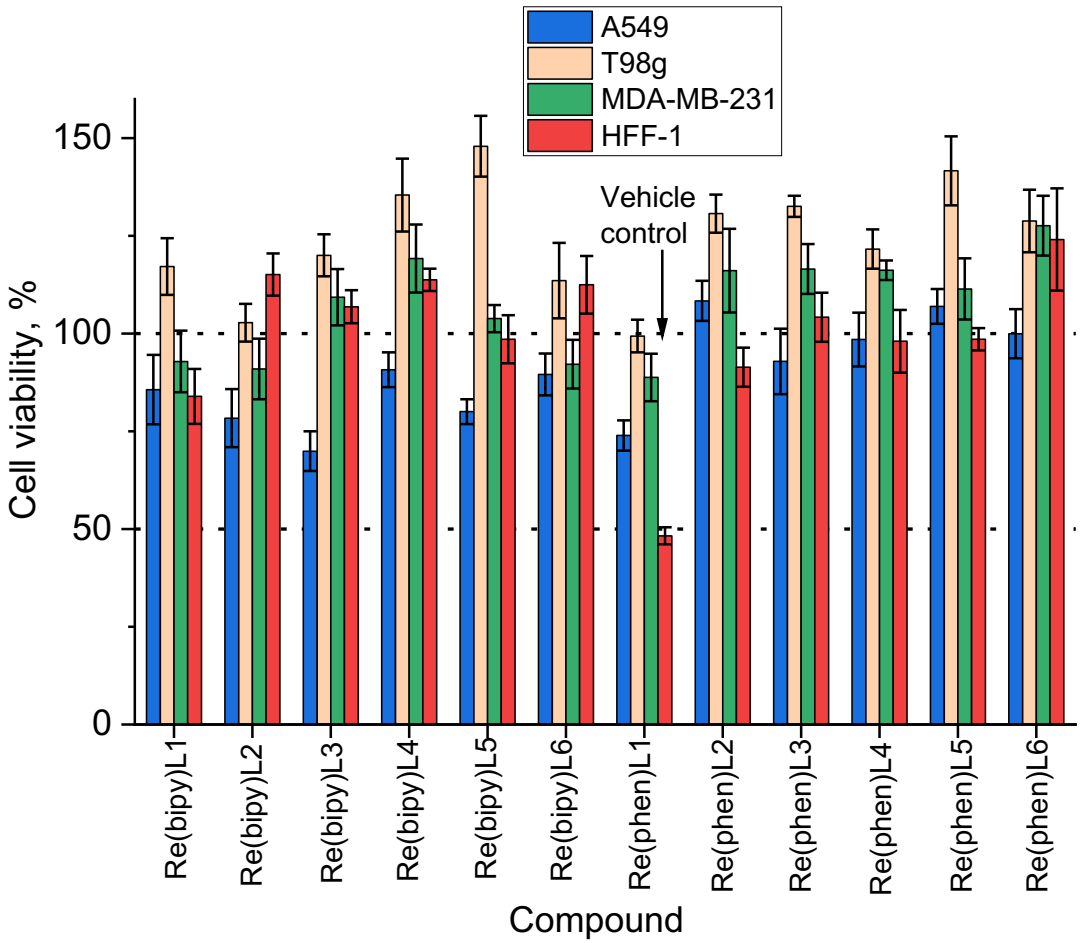

Figure S37 Comparison of anti-proliferative activities (MTT assays) of the Re(I) complexes (5.0 μM Re) in a panel of cancer and non-cancer cell lines in 72 h assays. Error bars represent mean values and standard deviations of two independent experiments, each including six replicate wells (n=12).

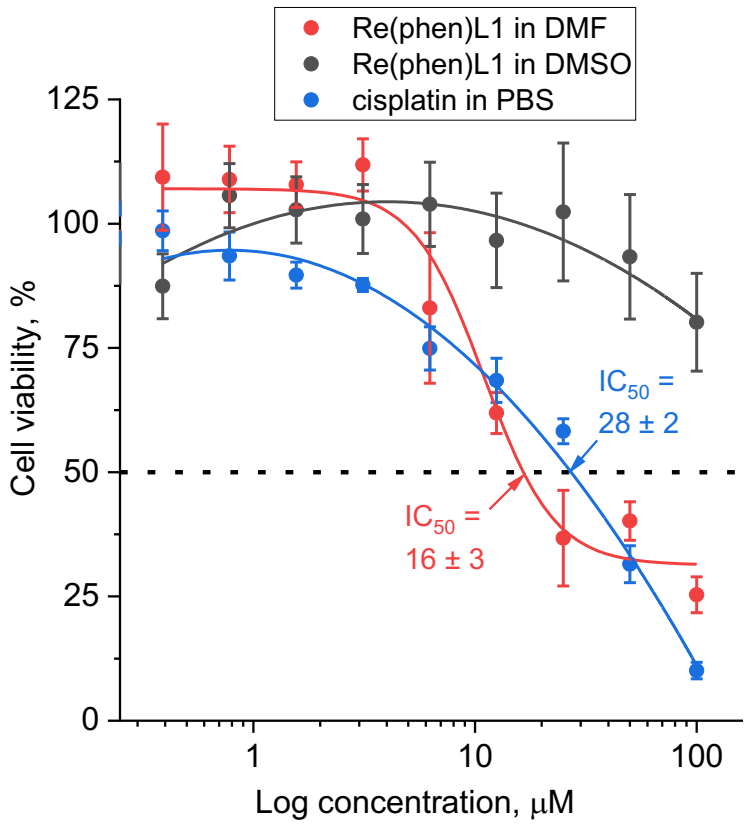

Figure S38 Comparison of concentration-viability curves for 72h assays in T98g cells for **Re(phen)L1** (using 10 mM stock solutions in DMF or DMSO) and cisplatin (using 1.0 mM stock solution in PBS). Points and error bars represent mean values and standard deviations of six replicate wells, and lines are sigmoidal or polynomial fits of experimental data.

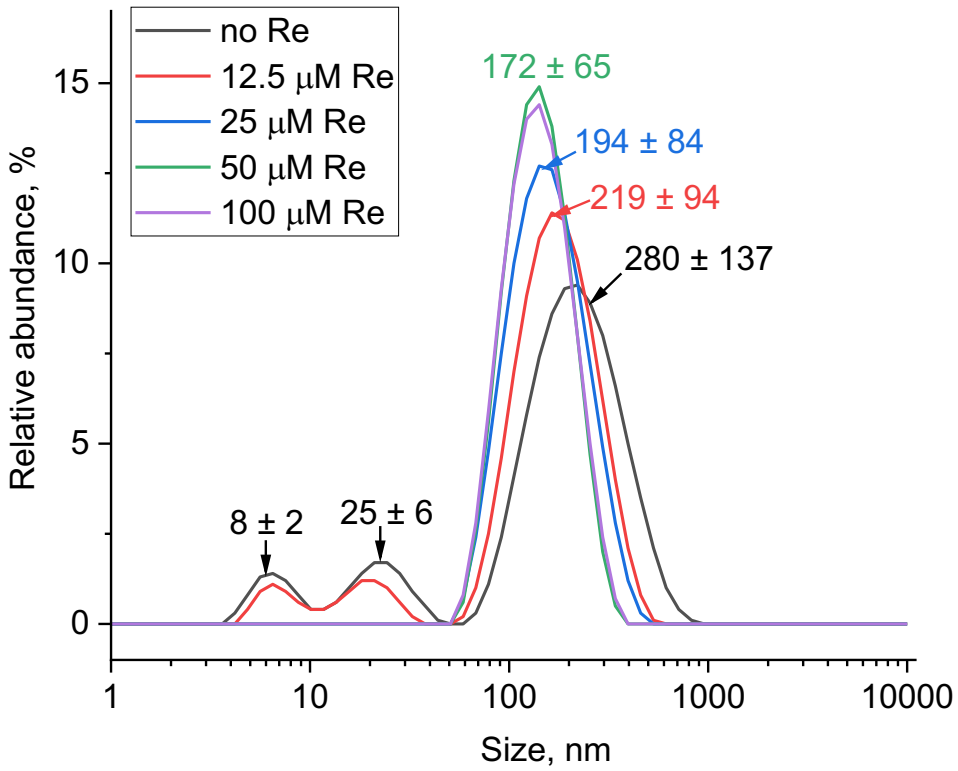

Figure S39 Changes in DLS profiles of cell culture medium (Advanced DMEM with 2% FCS) in the presence of increasing concentrations of **Re(phen)L1**. Media samples were incubated with **Re(phen)L1** for 2 h at 310 K before the measurements. DLS measurements were performed with a Malvern ZetaSizer NanoS instrument (173° scattering angle, 298 K) with ZEN0040 disposable cuvettes (Malvern Panalytical, Malvern, UK). Attribution of the peaks: 8 ± 2 nm and 25 ± 6 nm are due to proteins (predominantly albumin) contained in the medium; 280 ± 137 nm (in the absence of Re) is due to protein aggregates; 172 ± 65 nm (at high Re concentrations) is due to **Re(phen)L1** aggregates, and 219 ± 94 nm and 194 ± 84 nm (at lower Re concentrations) are due to a combination of protein and Re(phen)L1 aggregates. Note that the peak intensities depend on the particle size and are not proportionate to concentrations of the particles.